Mixed Proper Orthogonal Decomposition with Harmonic Approximation for Parameterized Order Reduction of Electromagnetic Models

# Mixed Proper Orthogonal Decomposition with Harmonic Approximation for Parameterized Order Reduction of Electromagnetic Models

Riccardo Torchio
*Dept. of Industrial Engineering*
*Università degli Studi di Padova*
Padova, Italy
riccardo.torchio@unipd.it

Alessandro Zanco
*Dept. of Electronics and Telecommunications*
*Politecnico di Torino*
Torino, Italy
alessandro.zanco@polito.it

Francesco Lucchini
*Centro Ricerche Fusione*
*Università degli Studi di Padova*
Padova, Italy
francesco.lucchini@studenti.unipd.it

Piergiorgio Alotto
*Dept. of Industrial Engineering*
*Università degli Studi di Padova*
Padova, Italy
piergiorgio.alotto@unipd.it

Stefano Grivet-Talocia
*Dept. of Electronics and Telecommunications*
*Politecnico di Torino*
Torino, Italy
stefano.grivet@polito.it

***Abstract*—This paper presents some preliminary investigations on a hybrid Model Order Reduction approach for parameter-dependent electromagnetic systems. Starting from an integral equation formulation of the field problem, we introduce a first level of compression based on the well-established Proper Orthogonal Decomposition (POD). The result is a small-scale approximation of the full-order discrete field formulation, which retains an explicit dependence on the set of free parameters defining the geometry. The evaluation of the reduced model for arbitrary parameter configurations remains very expensive, as it requires the construction of the full system equations before its projection onto a lower-dimensional space. This problem is solved by constructing a surrogate macromodel of the parameterized reduced-order system through a multivariate Fourier approximation. Numerical results applied to a moving coil over a finite ground plane show model compression above 99% while preserving accuracy on currents and fields within 1%.**

***Index Terms*—Proper Orthogonal Decomposition (POD), parameterized model-order reduction (PMOR), parametric geometry, integral equations.**

## I. Introduction

The design and the optimization of new generation electric and electronic devices often requires testing several geometrical configurations and mutual positions of different parts of the components, in order to select the best configuration that ensures overall good performances and Electromagnetic Compatibility (EMC) compliance. Such verification is performed by solving Maxwell's equations using appropriate numerical tools. Unfortunately, the computational cost of electromagnetic (EM) simulations for sophisticated and complex devices may be prohibitive when several configurations need to be tested.

Numerical methods that can reduce the computational cost of geometrical parametric analyses can be of great benefit. In the literature, several approaches have been proposed, e.g. the multiparameter moment matching model-reduction algorithm described in [1]. Other approaches that have been applied include [2], where Reduced-Order Modeling and discrete empirical interpolation are used, and [3], where a unifying projection-based framework for structure-preserving interpolatory model reduction is proposed. Several other methods based on Reduced Order Modeling and/or interpolation have been proposed in the literature for EM and non-EM problems, such as [4]–[10].

In this paper, with the aim of developing a tool for the automatic construction of computationally cheap and accurate parametric models of devices, we perform preliminary investigations on a hybrid Model Order Reduction approach for parameter-dependent electromagnetic systems. Starting from an integral equation formulation of the field problem which is derived from the well-known Partial Element Equivalent Circuit (PEEC) scheme [11], we introduce a first level of compression based on the well-established Proper Orthogonal Decomposition (POD). The result is a compact approximation of the full-order discrete field formulation, which retains an explicit dependence on the set of free parameters defining geometry. The evaluation of the reduced model for arbitrary parameter configurations remains very expensive, as it requires the construction of the full system equations before its projection onto a lower-dimensional space. This problem is solved by constructing a surrogate macromodel of the parameterized reduced-order system through a multivariate Fourier approximation. The result is an accurate compact yet fully parameterized model, which can be used for fast parameter sweep, optimization, and what-if analyses. The problem chosen for numerical experiments considers a coil moving over a finite ground plane. Despite its simplicity, the large geometrical variations have a strong influence on the local fields and current distributions. Therefore, this case study is a good candidate to test the performance of the proposed approach in terms of retained accuracy and model compression.

## II. Integral Formulation with Geometric Parameterization

### A. Overview of PEEC method

The selected integral equation formulation is based on the well-known Electric Field Integral Equation:

$$\mathbf{E}(\mathbf{r}) = -i\omega\mathbf{A}(\mathbf{r}) - \nabla\varphi(\mathbf{r}) + \mathbf{E}_{ext}(\mathbf{r}) \tag{1}$$

where $\mathbf{E}$ is the electric field, $\mathbf{A}$ is the magnetic vector potential, and $\varphi$ is the scalar electric potential. $\mathbf{E}_{ext}$ is the incident external field produced by the unperturbed source, $\mathbf{r}$ is the position, $i$ is the imaginary unit, and $\omega$ is the angular frequency. For simplicity, we will assume that $\mu_r = 1$ and $\varepsilon_r = 1$ everywhere. The computational domain includes conductive regions with finite conductivity, collectively denoted as $\Omega$.

Vector and scalar potentials in (1) are given by their integral expressions in terms of the current density vector $\mathbf{J}$ [12]. Equation above is then complemented by

$$\mathbf{E}(\mathbf{r}) = \rho(\mathbf{r})\mathbf{J}(\mathbf{r}), \text{ with } \mathbf{r} \in \Omega \tag{2}$$

where $\rho$ is the electric resistivity. Moreover, the continuity equation $\nabla \cdot \mathbf{J}(\mathbf{r}) = -i\omega\varrho(\mathbf{r})$ holds, where $\varrho$ is the charge density. Then, all conductive regions are meshed, and the current density $\mathbf{J}$ and the scalar potential $\varphi$ are expanded as in [12]. Applying a Galerkin projection scheme, the EM problem is approximated by the following linear system of equations

$$\begin{bmatrix} \mathbf{R} + i\omega\mathbf{L} & \mathbf{G} \\ \mathbf{P}\mathbf{G}^T & -i\omega\mathbf{1} \end{bmatrix} \begin{bmatrix} \mathbf{j} \\ \mathbf{\Phi} \end{bmatrix} = \begin{bmatrix} \mathbf{e_{ext}} \\ \mathbf{0} \end{bmatrix} \tag{3}$$

where $\mathbf{R}$, $\mathbf{L}$, and $\mathbf{P}$ are the (sparse) resistance, (dense) inductance, and (dense) potential matrices, respectively. Coefficients of such matrices are given in, e.g., [12]. In (3), $\mathbf{G}$ is the volumes–faces incidence matrix, whereas $\mathbf{e_{ext}}$ is the array corresponding to the incident external electric field. The problem described by (3) is usually interpreted as a fully coupled electric circuit with a very large number of components, where elements are the circuit nodes and the internal faces of the mesh (which connect two elements) are the circuit branches. Thus, $\mathbf{G}$ is the incidence matrix of this equivalent circuit.

### B. Parametrization

When the discretized geometry of the problem is described by some parameters (shapes, mutual position and orientation of conductors), $\mathbf{R}$, $\mathbf{L}$, and $\mathbf{P}$ in (3) exhibit, in principle, a dependence on such parameters, denoted as $\mathbf{d} = [d_1, \ldots, d_{N_d}]$ in the following.

### C. Problem statement

Without loss of generality, we assume that $\mathbf{e_{ext}}$ does not depend on the geometry (as in the case of lumped voltage source excitation), thus

$$\underbrace{\begin{bmatrix} \mathbf{R}(\mathbf{d}) + i\omega\mathbf{L}(\mathbf{d}) & \mathbf{G} \\ \mathbf{P}(\mathbf{d})\mathbf{G}^T & -i\omega\mathbf{1} \end{bmatrix}}_{\mathbf{S}(\mathbf{d})} \underbrace{\begin{bmatrix} \mathbf{j}(\mathbf{d}) \\ \mathbf{\Phi}(\mathbf{d}) \end{bmatrix}}_{\mathbf{x}(\mathbf{d})} = \underbrace{\begin{bmatrix} \mathbf{e_{ext}} \\ \mathbf{0} \end{bmatrix}}_{\mathbf{u}}. \tag{4}$$

Moreover, we also assume normalized parameters $\mathbf{d} \in \mathcal{D} \subset \mathbb{R}^{N_d}$, where $\mathcal{D}$ is a unit hypercube of dimension $N_d$. The size of system (4) will be denoted as $N$.

## III. Reduced-Order Modeling via Proper Orthogonal Decomposition

The full-scale parameterized PEEC system (4) may require excessive computational resources for carrying out parameter sweeps or design optimization. Therefore, we apply a POD algorithm [13] in order to reduce its complexity, with the main objective of deriving a Reduced-Order Model (pROM) that includes in a closed form an explicit, approximate yet error-controlled dependence on the parameters.

### A. Proper Orthogonal Decomposition

The main idea of POD schemes is to approximate the true solution through a suitable projection onto a small-dimensional subspace. This approximated solution is computed as the true (exact) solution of a reduced-size system (the pROM) obtained by projecting the full system (4) onto this subspace. The main steps of a standard POD algorithm are summarized in the following, where the projection basis $\mathbf{V}$ is iteratively constructed, until some stopping condition is attained. This condition is here specified in terms of a tolerance $\eta$ on the pROM accuracy with respect to the full system.

*a) Initialization*

Matrix $\mathbf{V}$ is initially empty. The process is initialized by choosing a candidate parameter value $\mathbf{d}$ to setup the iterations, here selected as the centroid of the parameter domain.

*b) Augmenting the POD basis*

For the candidate configuration $\mathbf{d}$, the solution $\mathbf{x}(\mathbf{d})$ of (4) is computed and used to augment the projection matrix $\mathbf{V}$. The latter is updated through a Gram-Schmidt Orthogonalization (GSO) process

$$\mathbf{V} \leftarrow \text{GSO}\left\{[\mathbf{V},\ \mathbf{x}(\mathbf{d})]\right\}. \tag{5}$$

In particular, the new vector $\mathbf{x}(\mathbf{d})$ is orthogonalized with respect to all preexisting basis vectors, normalized to have unit Euclidean norm, and appended as the last column. Matrix $\mathbf{V}$ is thus guaranteed to preserve orthonormality through iterations.

*c) Testing the POD basis*

Once the projection basis is available, its accuracy in representing the solution space of (4) for arbitrary parameter configurations is tested. To this end, a set of testing vectors $\mathcal{T} = \{\mathbf{d}_h \in \mathcal{D}, h = 1, \ldots, N_T\}$ are selected, and the provisional basis $\mathbf{V}$ is used to project the full order problem onto the basis for each of these testing vectors (the operator $^*$ denotes the conjugate transpose)

$$\mathbf{T}(\mathbf{d}) = \mathbf{V}^* \mathbf{S}(\mathbf{d})\, \mathbf{V}, \qquad \mathbf{d} \in \mathcal{T}. \tag{6}$$

$$\mathbf{z} = \mathbf{V}^* \mathbf{u}. \tag{7}$$

Matrix $\mathbf{T}(\mathbf{d})$ and right-hand side $\mathbf{z}$ provide the pMOR instantiated at $\mathbf{d} \in \mathcal{T}$. Then, the pMOR solution is

$$\mathbf{y}(\mathbf{d}) = \mathbf{T}(\mathbf{d})^{-1}\mathbf{z}, \quad \mathbf{d} \in \mathcal{T} \tag{8}$$

that is mapped to the corresponding full-size approximate solution $\hat{\mathbf{x}}(\mathbf{d})$ of the full order model, which is obtained as an element of the subspace spanned by the current basis

$$\hat{\mathbf{x}}(\mathbf{d}) = \mathbf{V}\,\mathbf{y}(\mathbf{d}), \quad \mathbf{d} \in \mathcal{T}. \tag{9}$$

Since this set of solutions are only approximations of the full system solutions, their accuracy is evaluated through the equation error (residual)

$$\Delta(\mathbf{d}) = \mathbf{S}(\mathbf{d})\hat{\mathbf{x}}(\mathbf{d}) - \mathbf{u}, \quad \mathbf{d} \in \mathcal{T}. \tag{10}$$

The worst-case residual

$$\Delta_\star = \max_{\mathbf{d}\in\mathcal{T}} \|\Delta(\mathbf{d})\| \tag{11}$$

is finally identified with the corresponding parameter configuration $\mathbf{d}_\star$.

*d) Stopping or Restarting*

If $\Delta_\star$ is larger than the prescribed tolerance $\eta$, then a new iteration of the algorithm is performed by selecting $\mathbf{d} = \mathbf{d}_\star$. Otherwise $\Delta_\star < \eta$, i.e. the pROM is uniformly accurate in the parameter space (at least over the testing set). The algorithm stops and the final pROM is returned. Note that at this stage the pROM is defined by the finalized projection basis $\mathbf{V} \in \mathbb{C}^{N\times q}$ together with the full system matrices $\mathbf{S}(\mathbf{d})$ and right-hand side $\mathbf{u}$. Evaluation of the pROM and its solution at any arbitrary $\mathbf{d} \in \mathcal{D}$ still requires the construction of the full system and its successive projection (6)-(7). It is expected that the finalized basis $\mathbf{V}$ is "tall and thin", with a number of columns $q$ (the basis elements) much smaller than the number of rows $N$ (the unknowns of the original full-scale PEEC system).

### B. Remarks

At each iteration, until convergence, the POD algorithm requires the expensive solution of the full order model (4), with an additional overhead for the construction of $N_T$ pROMs over the testing set for evaluating the residual (10) at each iteration. For the target application investigated in this work, a limited number of iterations is generally required (in the order of a few tens) in order to reach an accuracy $\eta = 10^{-4}$, using a testing set with $N_T = 20$. Once available, the pMOR can be used to solve the parametric domain problem for a generic value of $\mathbf{d} \in \mathcal{D}$. Unfortunately, due to the non-affine dependence of matrices $\mathbf{R}$ and $\mathbf{L}$ on the geometric parameters, the evaluation of the pMOR for an arbitrary parameter configuration $\mathbf{d}$ is very expensive, since it requires the construction of the full-order system, its projection onto the POD basis $\mathbf{V}$, and finally the actual solution in the reduced space (the latter requiring a negligible cost). It would be highly desirable to derive the reduced-order model for a given $\mathbf{d}$ *without* having to evaluate and project the corresponding full-order model.

In the following section, we show that a direct interpolation/approximation of the pROM or even of its solution in the reduced space dramatically reduces the computational cost of the entire process, without significantly impacting overall accuracy. The proposed approach follows the spirit of [14], with however different choices in the representation and interpolation of the parametric dependence of the pROM, as required by the present application.

## IV. Approximate Parameterization through Surrogate Macromodels

The POD procedure of Sec. III produces a global *parameter-independent* projection basis $\mathbf{V}$ which can be used to derive the pMOR

$$\mathbf{T}(\mathbf{d})\mathbf{y}(\mathbf{d}) = \mathbf{z} \tag{12}$$

via (6)-(7). The parameterization of (12) is however only formal, since the closed-form dependence on the pMOR matrix $\mathbf{T}(\mathbf{d})$ or its solution $\mathbf{y}(\mathbf{d})$ on $\mathbf{d}$ is unknown. A discrete set $\mathcal{H} \subset \mathcal{D}$ of $\rho = |\mathcal{H}|$ instances

$$(\widehat{\mathbf{T}}_h, \hat{\mathbf{y}}_h), \quad \widehat{\mathbf{T}}_h = \mathbf{T}(\mathbf{d}_h),\ \hat{\mathbf{y}}_h = \mathbf{y}(\mathbf{d}_h), \quad \mathbf{d}_h \in \mathcal{H} \tag{13}$$

can be produced by sampling the parameter space $\mathcal{D}$. The production of the samples (13) is however expensive, since it requires construction and projection of the full-order system.

For this preliminary investigation and throughout the following, we consider a set of training samples (13) to cover uniformly the parameter space $\mathcal{D}$, either as a uniform Cartesian grid (for small $N_d$) or according to a space-filling Sobol sequence (for large $N_d$). In addition, we introduce a set $\mathcal{V}$ of $N_V$ validation data samples, defined such that $\mathcal{V} \cap \mathcal{H} = \emptyset$.

The objective of this Section is to construct a *surrogate macromodel*

$$\widetilde{\mathbf{T}}(\mathbf{d})\tilde{\mathbf{y}}(\mathbf{d}) = \mathbf{z} \tag{14}$$

providing a closed-form representation of the true yet unknown pROM (12) through a suitable approximation of its parameter dependence. This is achieved by exploiting the training samples (13) and enforcing some interpolation, approximation or fitting condition on the pROM matrix

$$\widetilde{\mathbf{T}}(\mathbf{d}_h) \approx \widehat{\mathbf{T}}_h, \quad \mathbf{d}_h \in \mathcal{H} \tag{15}$$

or directly on its solution

$$\tilde{\mathbf{y}}(d_h) \approx \hat{\mathbf{y}}_h, \quad \mathbf{d}_h \in \mathcal{H}. \tag{16}$$

These two interpolation strategies are complementary:

- **direct:** using (16) requires the inversion of the pROM (12) only in the training phase to precompute the samples $\hat{\mathbf{y}}_h$ required to construct the macromodel; evaluation of the approximate full system solution $\tilde{\mathbf{x}}(\mathbf{d})$ for a given $\mathbf{d}$ requires only pre-multiplication by the projection matrix

$$\tilde{\mathbf{x}}(\mathbf{d}) = \mathbf{V}\tilde{\mathbf{y}}(\mathbf{d}) \tag{17}$$

- **two-step:** using (15) requires instead the approximation of $q \times q$ complex matrix entries during macromodel training, whereas instantiation of the pROM to evaluate the approximate full system solution $\tilde{\mathbf{x}}(\mathbf{d})$ for a given $\mathbf{d}$ requires the solution of the surrogate equations (14) (inversion of a $q \times q$ system) followed by (17).

Both strategies amount to constructing some closed-form approximate parametrization of a complex vector or a complex matrix, which can be performed elementwise. In the following,

we denote through the scalar $\vartheta(\mathbf{d}) \in \mathbb{C}$ any generic entry of matrix $\mathbf{T}(\mathbf{d})$ or vector $\mathbf{y}(\mathbf{d})$, with the corresponding training samples denoted as

$$\widehat{\vartheta}_h = \vartheta(\mathbf{d}_h), \quad \mathbf{d}_h \in \mathcal{H} \tag{18}$$

and the surrogate model as $\widetilde{\vartheta}(\mathbf{d})$, to be constructed such that

$$\widetilde{\vartheta}(\mathbf{d}_h) \approx \widehat{\vartheta}_h, \quad \mathbf{d}_h \in \mathcal{H}. \tag{19}$$

### A. Multidimensional Fourier approximation

In this work we assume the surrogate approximation $\widetilde{\vartheta}(\mathbf{d})$ to be defined as a multi-linear combination of parameter basis functions $B_{\boldsymbol{\ell}}(\mathbf{d})$, as

$$\begin{aligned}\widetilde{\vartheta}(\mathbf{d}) &= \sum_{\boldsymbol{\ell}} \widetilde{\vartheta}_{\boldsymbol{\ell}} B_{\boldsymbol{\ell}}(\mathbf{d}) \\ &= \sum_{\ell_1=0}^{\bar{\ell}_1} \cdots \sum_{\ell_{N_d}=0}^{\bar{\ell}_{N_d}} \widetilde{\vartheta}_{\ell_1,\ldots,\ell_{N_d}} B_{\ell_1}(d_1) \times \cdots \times B_{\ell_{N_d}}(d_{N_d})\end{aligned} \tag{20}$$

where $\ell_\nu$ provides indexing for univariate basis functions along dimension $\nu$ up to order $\bar{\ell}_\nu$, and multi-index $\boldsymbol{\ell}$ collects all individual indices $\ell_\nu$. For simplicity, without loss of generality, we assume the expansion orders to be equal $\bar{\ell}_1 = \cdots = \bar{\ell}_{N_d} = \bar{\ell}$. The multivariate basis set is obtained as a Cartesian product of univariate bases.

In order to guarantee an accurate parameterized approximation (19), particular care should be taken to the selection of the multivariate basis $B_{\boldsymbol{\ell}}(\mathbf{d})$. Given the observed smoothness of both pROM matrix and its solution, we adopt a trigonometric (*Fourier*) polynomial basis, which has been verified to provide accurate results. Hence, we define the basis functions as

$$\begin{cases} B_0(\mathbf{d}) = 1, \\ B_\ell(\mathbf{d}) = \cos(2\pi\lceil \ell/2 \rceil \mathbf{d}), \quad \ell = 1, 3, 5, \ldots \\ B_\ell(\mathbf{d}) = \sin(2\pi\lceil \ell/2 \rceil \mathbf{d}), \quad \ell = 2, 4, 6, \ldots \end{cases} \tag{21}$$

The tensor collecting all multi-linear expansion coefficients $\widetilde{\vartheta}_{\boldsymbol{\ell}}$ is computed by enforcing the fitting condition (19) in least squares sense. Once the $q$ (or $q^2$) estimates (20) are available for all elements of either pROM matrix $\widetilde{\mathbf{T}}(\mathbf{d})$ or its solution $\tilde{\mathbf{y}}(\mathbf{d})$, we can assemble the macromodel (14), whose elementwise evaluation through (20) amounts to a simple (small-size) multivariate vector or matrix function evaluation.

### B. Error analysis

Both the POD process and the parameterized surrogate model introduce approximation errors that must be kept under control. Assuming $Q$ to be a placeholder for any scalar, vector and matrix variable, we define the following absolute $E^a_Q(\mathbf{d})$ and relative $E^r_Q(\mathbf{d})$ error metrics

$$E^a_Q(\mathbf{d}) = \left\| \tilde{Q}(\mathbf{d}) - Q(\mathbf{d}) \right\|, \quad E^r_Q(\mathbf{d}) = \frac{E^a_Q(\mathbf{d})}{\|Q(\mathbf{d})\|} \tag{22}$$

For later use, we introduce an additional overall (validation) relative error metric $\bar{E}^r_Q$, defined as

$$\bar{E}^r_Q = \max_{\mathbf{d} \in \mathcal{V}} E^r_Q(\mathbf{d}) \tag{23}$$

**IV-B1 Surrogate macromodeling error —** We first analyze the error $E^a_{\mathbf{y}}(\mathbf{d})$ introduced by the parameterized surrogate approximation. Depending on the strategy used to build the surrogate model two scenarios arise:

- in case we directly approximate the reduced solutions, as in (16), we have a direct control over $E^a_{\mathbf{y}}(\mathbf{d})$ since it coincides with the least squares residual.
- in case, we approximate the reduced system matrix, as in (15) we can only provide an upper bound on $E^a_{\mathbf{y}}(\mathbf{d})$. Recalling that the condition number $\kappa(\mathbf{d})$ of $\mathbf{T}(\mathbf{d})$ provides the following inequality

$$E^r_{\mathbf{y}}(\mathbf{d}) \leq \kappa(\mathbf{d}) E^r_{\mathbf{T}}(\mathbf{d}) \tag{24}$$

we can write

$$E^a_{\mathbf{y}}(\mathbf{d}) \leq \kappa(\mathbf{d}) \, \|\mathbf{y}(\mathbf{d})\| \, E^r_{\mathbf{T}}(\mathbf{d}). \tag{25}$$

An accurate approximation of the reduced matrix is not sufficient; we should also ensure the condition number $\kappa(\mathbf{d})$ to be small.

**IV-B2 From reduced to full space —** Next we consider the propagation of an approximation error from the reduced space to the full-size space. Defining the error on the full system solution induced by the surrogate approximation as $E^a_{\tilde{\mathbf{x}}}(\mathbf{d})$ and recalling that the mapping from the reduced to the full space is provided by the POD projection matrix $\mathbf{V}$ through (17) and (9), we have

$$E^a_{\tilde{\mathbf{x}}}(\mathbf{d}) = \|\mathbf{V}\tilde{\mathbf{y}}(\mathbf{d}) - \mathbf{V}\mathbf{y}(\mathbf{d})\| = E^a_{\mathbf{y}}(\mathbf{d}) \tag{26}$$

since $\mathbf{V}^T\mathbf{V} = \mathbf{I}$.

**IV-B3 Combined approximation error —** Finally we estimate the overall reconstruction error $E^a_{\mathbf{x}}(\mathbf{d})$ by combining the effects of surrogate macromodeling and POD approximation. Using (26) and applying the triangle inequality leads to

$$E^a_{\mathbf{x}}(\mathbf{d}) \leq \|\hat{\mathbf{x}}(\mathbf{d}) - \mathbf{x}(\mathbf{d})\| + E^a_{\mathbf{y}}(\mathbf{d}) \tag{27}$$

Further manipulations lead to

$$\begin{aligned} E^a_{\mathbf{x}}(\mathbf{d}) &\leq \left\| \mathbf{S}^{-1}(\mathbf{d})\mathbf{S}(\mathbf{d})\big(\hat{\mathbf{x}}(\mathbf{d}) - \mathbf{x}(\mathbf{d})\big) \right\| + E^a_{\mathbf{y}}(\mathbf{d}) \\ &\leq \left\| \mathbf{S}^{-1}(\mathbf{d}) \right\| \left\| \mathbf{S}(\mathbf{d})\big(\hat{\mathbf{x}}(\mathbf{d}) - \mathbf{x}(\mathbf{d})\big) \right\| + E^a_{\mathbf{y}}(\mathbf{d}) \end{aligned} \tag{28}$$

The term $\left\| \mathbf{S}(\mathbf{d})\big(\hat{\mathbf{x}}(\mathbf{d}) - \mathbf{x}(\mathbf{d})\big) \right\|$ is the pMOR error residual $\Delta(\mathbf{d})$ defined in (10) that, assuming the POD process reached uniform convergence, is bounded by $\eta$. To conclude, the following bound holds for the overall reconstruction error

$$E^a_{\mathbf{x}}(\mathbf{d}) \leq \left\| \mathbf{S}(\mathbf{d})^{-1} \right\| \eta + E^a_{\mathbf{y}}(\mathbf{d}) \tag{29}$$

## V. Experiments

In this Section, we apply both direct and two-step surrogate macromodeling approaches to a benchmark problem, with the aim of assessing and comparing their performance. Our test bench is a simple academic problem, i.e., a square spiral copper coil placed above a square aluminium plate in the $xy$-plane, see Fig. 1. The coil is excited with a current source of 1 A at 1 MHz and the displacements along the $x$ and $y$

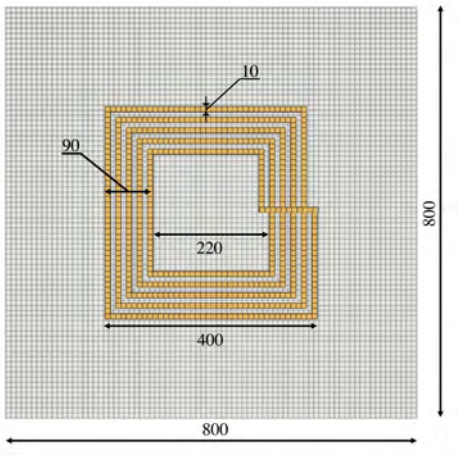


Fig. 1: Models of the square coil and aluminium plate ($xy$ view). Dimensions are in $\mu$m.

axes between the plate and the coil are the two geometric parameters chosen in this analysis. The copper traces and the aluminium plate have both a 4 $\mu$m thickness and the distance along the $z$ axis between the square coil and the aluminium plate is 48 $\mu$m. The full PEEC system size is $N = 20289$, with 13264 currents and 7025 potentials. With reference to Fig. 1, the maximum displacement of the square coil along the $x$ and $y$ axes is $\pm 150$ $\mu$m. The POD algorithm has been applied with a stopping threshold $\eta = 10^{-4}$. At convergence, $q = 43$ reduced bases have been selected to achieve the desired accuracy. The resulting pMOR has been processed by the proposed multidimensional Fourier approximation for the construction of the parameterized surrogate, using both direct and two-step approaches.

Figure 2 shows the relative RMS validation error of the two surrogates for an increasingly large number of harmonics. In both cases, as expected, the error decreases monotonically as the number of harmonics increases, reaching a smaller error when approximating the pROM matrix with respect to its solution. The dependence of the reduced matrix $\mathbf{T}(\mathbf{d})$ on geometrical parameters is expected to be smooth and of the same type as in the full PEEC system (4). Conversely, the solution $\mathbf{y}(\mathbf{d})$ is obtained after matrix inversion, hence its parameter dependence is affected by the induced variations on $\mathbf{T}^{-1}(\mathbf{d})$. These considerations are confirmed by Fig. 3, where representative elements of the parameterized POD matrix (top panel) and its solution (bottom panel) are depicted in the top and bottom panel, respectively. Total variations of the solution exhibit more structure and require consequently a larger number of harmonics for their accurate approximation.

Based on the results of Figure 2, we select order 6 and 10 in the Fourier approximation for the two-step and the direct method, respectively, and we perform a detailed investigation on the achieved accuracy. Table I reports the RMS and maximum errors for each approximation step and for both surrogate modeling methods. The worst-case error on the full-size solution $\bar{E}^r_{\mathbf{x}}$ is at most 3.2%, which is remarkable considering

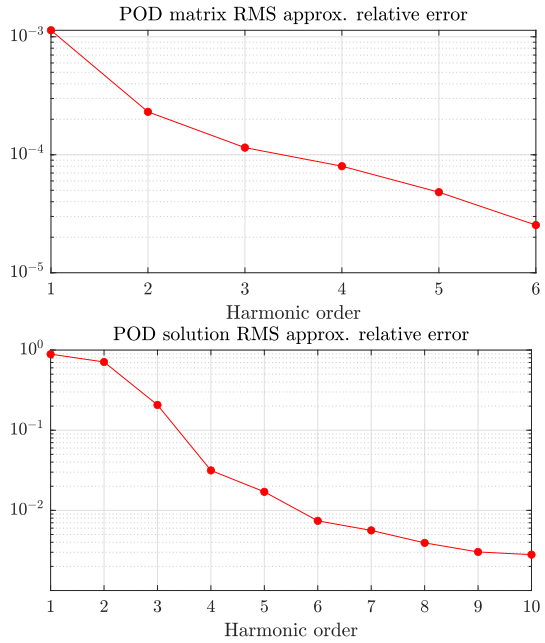


Fig. 2: Testing the convergence properties of the multidimensional Fourier approximation. Top panel: two-step method (approximation of $\mathbf{T}(\mathbf{d})$). Bottom panel: direct method (approximation of $\mathbf{y}(\mathbf{d})$).

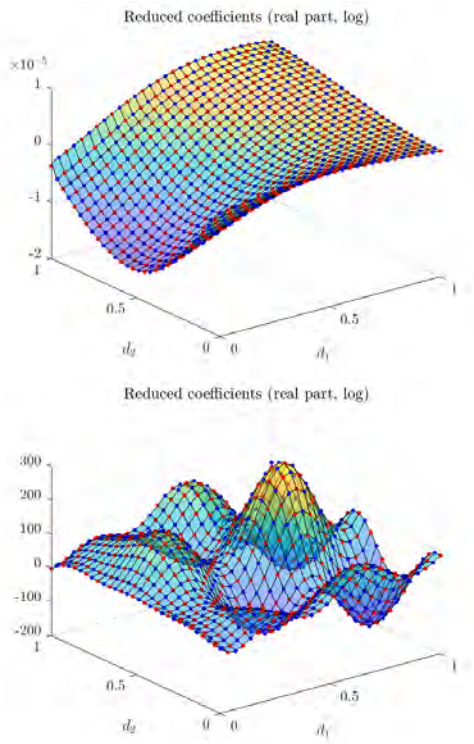


Fig. 3: Parameter dependence of a representative element of the pROM matrix $\mathbf{T}(\mathbf{d})$ (top) and pROM solution $\mathbf{y}(\mathbf{d})$ (bottom). Raw data are represented with colored surfaces, while red and blue dots represent the surrogate model evaluated on training and validation samples, respectively.

TABLE I: Approximation Errors Achieved by Proposed Hybrid POD/Surrogate Macromodeling Approach

| Error | Method | Max (%) | RMS (%) |
|---|---|---|---|
| $\bar{E}^r_{\mathbf{T}}$ | Two-step | $9.2 \cdot 10^{-3}$ | $2.5 \cdot 10^{-3}$ |
| $\bar{E}^r_{\mathbf{x}} = \bar{E}^r_{\mathbf{y}}$ | Two-step | 6.1 | 0.81 |
| | Direct | 3.4 | 0.3 |
| $\bar{E}^r_{\mathbf{x}}$ | Two-step | 3.2 | 1.4 |
| | Direct | 0.12 | 0.26 |

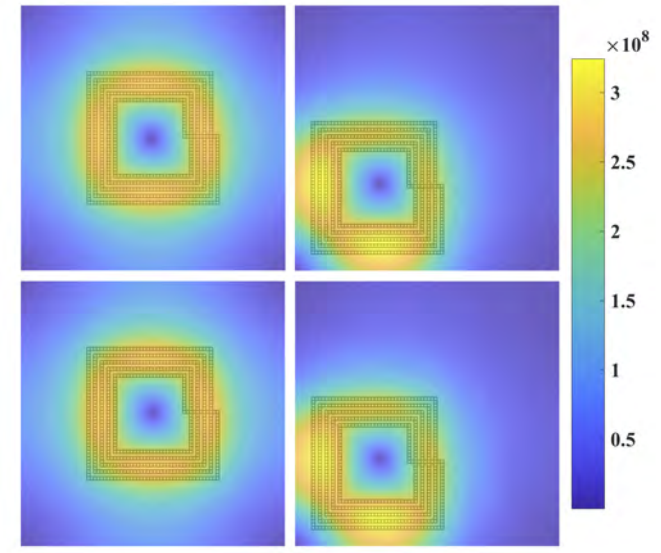


Fig. 4: Eddy currents (magnitude) on the aluminium plate. Top panels: True solution. Bottom panels: Solution derived from the direct surrogate macromodeling method. Left panels: $\mathbf{d} = [0, 0]$. Right panels: $\mathbf{d} = [-1, -1]$. Results are in A/m$^2$.

the various approximation steps and the aggressive compression ratio $q/N \approx 0.21\%$ of the pROM. Furthermore, the RMS errors are consistently below $1\%$. The largest error arises in the two-step method when computing the reduced POD solution vector through (14), with a worst-case error $\bar{E}^r_{\mathbf{y}} = 6.1\%$.

Finally, Figure 4 shows the magnitude of the eddy currents in the aluminium plate obtained from the direct solution of the full order system (4) (top panels) and from the direct method (bottom panels) for two different positions of the square coil. As can be noted, surrogate results are in very good agreement with reference solutions.

## VI. Conclusions

In this paper, some preliminary investigations of a hybrid Model Order Reduction approach for parameter-dependent electromagnetic systems have been presented. Starting from an integral equation formulation based on the Partial Element Equivalent Circuit method, we introduced a first level of compression based on the well-established Proper Orthogonal Decomposition. The result is a compact approximation of the full-order discrete field formulation, which retains an explicit dependence on the set of free parameters defining the geometry. Then, in order to obtain computationally cheap parametric model, a surrogate macromodel of the parameterized reduced-order system was constructed through a multivariate Fourier approximation. Numerical results applied to a moving coil over a finite ground plane show model compression above 99% while preserving accuracy on currents and fields within 1%. Although preliminary, the results presented in this paper may be of interest for software developers who want to implement tools for the automatic construction of computationally cheap and accurate parametric models of electromagnetic devices. Indeed, if such as procedure is embedded into an electromagnetic simulation software, designers would be able to generate computationally cheap and accurate parametric models without caring about the underlying theory and numerical procedures.

## References


[1] L. Daniel, O. C. Siong, L. Chay, K. H. Lee, and J. White, "A multi-parameter moment-matching model-reduction approach for generating geometrically parameterized interconnect performance models," *IEEE Transactions on Computer-Aided Design of Integrated Circuits and Systems*, vol. 23, no. 5, pp. 678–693, 2004.

[2] A. Nouri, E. Gad, B. Nouri, and M. Nakhla, "Parameterized Periodic Steady-State Analysis via Reduced-Order Modeling," *IEEE Transactions on Microwave Theory and Techniques*, vol. 69, no. 11, pp. 4599–4612, 2021.

[3] U. Baur, C. Beattie, P. Benner, and S. Gugercin, "Interpolatory Projection Methods for Parameterized Model Reduction," *SIAM Journal on Scientific Computing*, vol. 33, no. 5, pp. 2489–2518, 2011.

[4] J. Degroote, J. A. Vierendeels, and K. E. Willcox, "Interpolation among reduced-order matrices to obtain parameterized models for design, optimization and probabilistic analysis," *International Journal for Numerical Methods in Fluids*, vol. 63, pp. 207–230, 2009.

[5] S. Essahli, Y. Tao, F. Ferranti, M. Nakhla, and C. Person, "Multilevel Parameterized Model Order Reduction for Variability Analysis of Circuits," in *2021 IEEE MTT-S International Microwave Symposium (IMS)*, 2021, pp. 241–243.

[6] C. Yuan and T. Bechtold, "Geometrically Parametrized Reduced Order Model of a Miniaturized Thermoelectric Generator for Electrically Active Implants," in *2021 22nd International Conference on Thermal, Mechanical and Multi-Physics Simulation and Experiments in Microelectronics and Microsystems (EuroSimE)*, 2021, pp. 1–4.

[7] C. Yuan, D. Hohlfeld, and T. Bechtold, "Design optimization of a miniaturized thermoelectric generator via parametric model order reduction," *Microelectronics Reliability*, vol. 119, p. 114075, 2021.

[8] Z. Li, Y.-L. Jiang, and H. liang Mu, "Parametric model order reduction based on parallel tensor compression," *International Journal of Systems Science*, vol. 52, no. 11, pp. 2201–2216, 2021.

[9] B. Fröhlich, J. Gade, F. Geiger, M. Bischoff, and P. Eberhard, "Geometric element parameterization and parametric model order reduction in finite element based shape optimization," *Computational Mechanics*, vol. 63, no. 5, pp. 853–868, May 2019.

[10] L. Lombardi, Y. Tao, B. Nouri, F. Ferranti, G. Antonini, and M. S. Nakhla, "Parameterized model order reduction of delayed peec circuits," *IEEE Transactions on Electromagnetic Compatibility*, vol. 62, no. 3, pp. 859–869, 2020.

[11] A. Ruehli, G. Antonini, and L. Jiang, *Circuit Oriented Electromagnetic Modeling Using the Peec Techniques*. John Wiley & Sons, Ltd, 2017.

[12] R. Torchio, "A Volume PEEC Formulation Based on the Cell Method for Electromagnetic Problems From Low to High Frequency," *IEEE Transactions on Antennas and Propagation*, vol. 67, no. 12, pp. 7452–7465, 2019.

[13] A. Chatterjee, "An introduction to the proper orthogonal decomposition," *Current Science*, vol. 78, no. 7, pp. 808–817, 2000.

[14] J. Degroote, J. Vierendeels, and K. Willcox, "Interpolation among reduced-order matrices to obtain parameterized models for design, optimization and probabilistic analysis," *International Journal for Numerical Methods in Fluids*, vol. 63, no. 2, pp. 207–230, 2010.